PHYSICAL REVIEW A **84**, 020304(R) (2011)

Extremal quantum correlations: Experimental study with two-qubit states

A. Chiuri,[1,2] G. Vallone,[1,3,*] M. Paternostro,[4] and P. Mataloni[1,2]

[1]*Dipartimento di Fisica, Sapienza Università di Roma, Piazzale Aldo Moro 5, I-00185 Roma, Italy*

[2]*Istituto Nazionale di Ottica (INO-CNR), L.go E. Fermi 6, I-50125 Firenze, Italy*

[3]*Museo Storico della Fisica e Centro Studi e Ricerche Enrico Fermi, Via Panisperna 89/A, Compendio del Viminale, I-00184 Roma, Italy*

[4]*Centre for Theoretical Atomic, Molecular, and Optical Physics, School of Mathematics and Physics, Queen's University, Belfast BT7 1NN, United Kingdom*

(Received 25 March 2011; published 30 August 2011)

We explore experimentally the space of two-qubit quantum-correlated mixed states, including frontier states as defined by the use of quantum discord and von Neumann entropy. Our experimental setup is flexible enough to allow for high-quality generation of a vast variety of states. We address quantitatively the relation between quantum discord and a recently suggested alternative measure of quantum correlations.

DOI: 10.1103/PhysRevA.84.020304 PACS number(s): 03.67.Bg, 42.50.Dv, 42.50.Ex

Entanglement, "the characteristic trait of quantum mechanics" according to Schrödinger [1], is recognized as the key resource in the processing of quantum information and an important tool for the implementation of quantum communication and quantum-empowered metrology [2]. However, entanglement does not embody the unique way in which quantum correlations (QCs) can be set among the elements of a composite system. When generic mixed states are considered, QCs are no longer synonymous of entanglement: Other forms of stronger-than-classical correlations exist and can be enforced in the mixed state of a system. However, a general consensus on the measure of quantum correlations is still far from having been found. Among the quantifiers proposed so far, quantum discord [3] ($\mathcal{D}$) occupies a prominent position and enjoys a growing popularity within the community working on quantum information science due to its alleged relevance in the model for deterministic quantum computation with one qubit [4,5], extendibility to some important classes of infinite-dimensional systems [6], and peculiar role in open-system dynamics [7]. Recently, some attempts at providing an operational interpretation to discord have been reported [8].

Yet, interesting alternatives to discord exist, each striving at capturing different facets of QCs [9]. In Ref. [10], in particular, a measure based on the concept of perturbation of a bipartite quantum state [9] induced by joint local measurements has been put forward and extensively analyzed. Such an indicator, dubbed "ameliorated measurement-induced disturbance" (AMID), has been shown to faithfully signal fully classical states (i.e., states endowed with only classical correlations). AMID embodies an interesting upper bound to the nonclassicality content quantified by $\mathcal{D}$ and, at variance with the latter, is naturally symmetric.

A landmark in the study of quantum entanglement has been set by the identification of states maximizing the degree of two-qubit entanglement at set values of the global state mixedness [11]. This has spurred an extensive investigation of the interplay between entanglement and mixedness, which has culminated in the experimental exploration of the two-qubit entropic plane, including maximally entangled mixed states (MEMS), by a number of groups worldwide [12]. Needless to say, given the strong interplay between nonclassical correlations and mixedness, an experimental characterization analogous to the one performed for MEMS is not only highly desirable but also extremely interesting. This is precisely the aim of this work: Building on the framework provided by the theoretical studies in Refs. [10,13], here we experimentally navigate the space of two-qubit discorded states, focusing our attention, in particular, on the class of two-qubit maximally nonclassical mixed states (MNCMS); that is, those states maximizing the degree of quantum discord at assigned values of their global von Neumann entropy (VNE). We show a very good agreement between theoretical predictions and experimental evidence across the whole range of values of VNE for two-qubit states. Our extensive study comprises the generation and analysis of many quantum-correlated two-qubit states, from Werner states to MEMS associated with the relative entropy of entanglement and VNE [11].

Technically, this has been possible due to the high flexibility of the experimental setup used for our demonstration, which makes clever and effective use of the possibilities offered by well-tested sources for hyperentangled polarization-path photonic states. We engineer mixedness in the joint polarization state of two photonic qubits by tracing out the path degree of freedom (DOF). The properties of such residual states are then analyzed by means of the quantum state tomography (QST) toolbox [14], and a quantitative comparison between their quantum-correlation contents and the predictions on MNCMS is performed. The quality of the generated states is such that we have been able to experimentally verify the predictions given in Ref. [10] relating discord and AMID: We have generated the states embodying both the lower and upper bound to AMID at set values of discord. Our study should be regarded as the counterpart, dealing with the much broader context of general quantum correlations, of the seminal experimental investigations on the relation between entanglement and mixedness performed in Refs. [12]. As such, it encompasses an important step in the characterization of nonclassicality in general two-qubit states.

Resource-state generation. Before exploring the entropic two-qubit space, it is convenient to introduce the experimental

*Present Address: Department of Information Engineering, University of Padova, I-35131 Padova, Italy.

techniques used in order to achieve the ample variety of states necessary for our investigation. The key element for the state engineering in our setup is embodied by the state

$$|\xi\rangle_{AB} = \sqrt{1-\epsilon}|r\ell\rangle_{AB}|\phi^+(p)\rangle_{AB} + \sqrt{\epsilon}|\ell r\rangle_{AB}|HV\rangle_{AB}, \quad (1)$$

with $|\phi^\pm(p)\rangle_{AB} = \sqrt{p}|HH\rangle_{AB} \pm \sqrt{1-p}|VV\rangle_{AB}$. In Eq. (1), four qubits are encoded in the polarization and path DOFs of optical modes A and B. In particular, H (V) represents horizontal (vertical) polarization of a photon, while r (ℓ) is the right (left) mode in which each photon can be emitted from our source of entangled photon states, which we now describe. State $|\xi\rangle_{AB}$ is produced by suitably adapting the polarization-momentum source of hyperentangled states that has been recently used as basic building blocks in experimental test-beds on multipartite entanglement [15,16]. To generate $|\phi^+(p)\rangle$, a uv laser impinges back and forth on a nonlinear crystal [cf. Fig. 1(a)]. The forward emission generates the $|HH\rangle$ contribution. A quarter-wave plate (QWP_1) transforms the $|HH\rangle$ backward emission into $|VV\rangle$ after reflection at the spherical mirror M. The relative phase between the $|VV\rangle$ and $|HH\rangle$ contributions is changed by translating M. The weight $\sqrt{p}$ in the unbalanced Bell state $|\phi^+(p)\rangle_{AB}$ can be varied by rotating the quarter-wave plate $QWP_2[p]$ near M [see Fig. 1 (a)], which twice intercepts the uv pump beam. For more details on the generation of nonmaximally entangled states of polarization, see Ref. [17]. A four-hole mask allows us to select four longitudinal spatial modes (two per photon); namely, $|r\rangle_{A,B}$ and $|\ell\rangle_{A,B}$, within the emission cone of the crystal. The state thus produced reads $|\mathrm{HE}(p)\rangle = (|r\ell\rangle_{AB} + e^{i\gamma}|\ell r\rangle_{AB}) \otimes |\phi^+(p)\rangle_{AB}/\sqrt{2}$.

State $|\xi\rangle_{AB}$ has been obtained by making three further changes to $|\mathrm{HE}(p)\rangle$ [cf. Fig. 1 (a)]. First, the contributions of modes $|\ell r\rangle$ corresponding to the V cone is intercepted by inserting two beam stops. An attenuator is then placed on mode $|r\rangle_B$ so as to vary the relative weight between $|\ell r\rangle_{AB}$ and $|r\ell\rangle_{AB}$. This effectively corresponds to changing ϵ. Finally, an HWP [labelled HWP_1 in Fig. 1(a)], oriented at 45° and intercepting mode $|r\rangle_B$, allows the transformation $|\ell r\rangle|HH\rangle \rightarrow |\ell r\rangle|HV\rangle$. This gives the second term in Eq. (1), which we use to span the set of states relevant to our study.

Experimental navigation. We now introduce the measures of QCs considered in our work and discuss the results of our experimental investigation. We start with the reminder that discord is associated to the discrepancy between two classically equivalent versions of mutual information [3]. For a bipartite state ρ_{AB} the latter is defined as $\mathcal{I}(\rho_{AB}) = \mathcal{S}(\rho_A) + \mathcal{S}(\rho_B) - \mathcal{S}(\rho_{AB})$. Here, $\mathcal{S}(\rho) = -\mathrm{Tr}[\rho \log_2 \rho]$ is the VNE of the arbitrary two-qubit state ρ and ρ_j is the reduced density matrix of party $j = A,B$. One can also consider the expression $\mathcal{J}^{\leftarrow}(\rho_{AB}) = \mathcal{S}(\rho_A) - \mathcal{H}_{\{\hat{\Pi}_i\}}(A|B)$ (the one-way classical correlation [3]) with $\mathcal{H}_{\{\hat{\Pi}_i\}}(A|B) \equiv \sum_i p_i \mathcal{S}(\rho^i_{A|B})$ being the quantum conditional entropy associated with the the postmeasurement density matrix $\rho^i_{A|B} = \mathrm{Tr}_B[\hat{\Pi}_i \rho_{AB}]/p_i$ obtained upon performing the complete projective measurement $\{\Pi_i\}$ on system B ($p_i = \mathrm{Tr}[\hat{\Pi}_i \rho_{AB}]$). We define discord as $\mathcal{D}^{\leftarrow} = \inf_{\{\Pi_i\}}[\mathcal{I}(\rho_{AB}) - \mathcal{J}^{\leftarrow}(\rho_{AB})]$, where the infimum is calculated over the set of projectors $\{\hat{\Pi}_i\}$. Discord is, in general, asymmetric ($\mathcal{D}^{\leftarrow} \neq \mathcal{D}^{\rightarrow}$), with $\mathcal{D}^{\rightarrow}$ obtained by swapping the roles of A and B. This is at the origin of the possibility to distinguish between quantum-quantum states having $(\mathcal{D}^{\leftarrow},\mathcal{D}^{\rightarrow}) \neq 0$, quantum-classical states, classical-quantum states, which are states having one of the two values of discord strictly null, and, finally, classical-classical states for which $\mathcal{D}^{\leftarrow},\mathcal{D}^{\rightarrow} = 0$, which are bipartite states that simply embed a classical probability distribution in a two-qubit state [18]. The asymmetry inherent in discord would lead us to mistake a quantum-classical state for a classical state. In order to bypass such an ambiguity we will consider the symmetrized discord $\mathcal{D}^{\leftrightarrow} = \max[\mathcal{D}^{\leftarrow},\mathcal{D}^{\rightarrow}]$, which is zero only for classical-classical states.

AMID has been introduced as an alternative indicator of QCs as $\mathcal{A} = \mathcal{I}(\varrho_{AB}) - \mathcal{I}_c(\varrho_{AB})$ [10], where $\mathcal{I}_c(\varrho_{AB}) \equiv \sup_{\{\hat{\Omega}\}}\mathcal{I}(\varrho^{\hat{\Omega}}_{AB})$ and $\varrho^{\hat{\Omega}}_{AB}$ is the state resulting from the application of the arbitrary complete projective measurements $\hat{\Omega}_{kl} = \hat{\Pi}_{A,k} \otimes \hat{\Pi}_{B,l}$. Such a definition is motivated by the study in Ref. [19], where $\mathcal{I}_c$ is the classical mutual information (optimized over projective measurements), which is a symmetric measure of bipartite classical correlations. $\mathcal{A}$ is thus

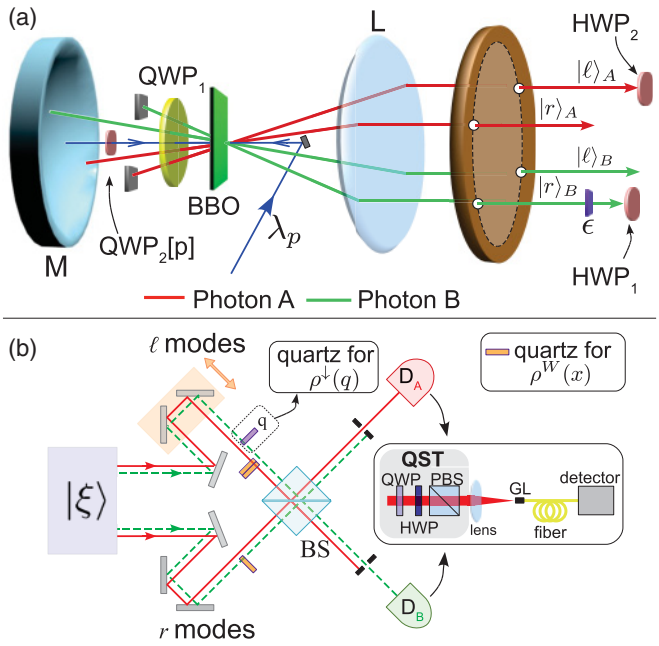

FIG. 1. (Color online) (a) Setup for the generation of a polarization-path 4-qubit entangled state. A Type-I nonlinear β-barium-borate crystal (BBO) is pumped by a vertically polarized uv laser at wavelength λ_p in a double-pass configuration. This produces nonmaximally entangled polarization states that, through the quarter-wave plates QWP_1 and QWP_2 (QWP_1 and QWP_2 are quarter-wave plates for $2\lambda_p$ and λ_p, respectively) and mirror M, can be turned into $|\phi^+(p)\rangle_{AB}$ (cf. the body of the paper). The four-hole mask selects four longitudinal spatial modes within the emission cone of the BBO crystal. The attenuator ϵ and the half-wave plates HWP_1 and HWP_2 allow the engineering of the polarization-path entangled state $|\xi\rangle_{AB}$. (b) Interferometer needed to perform the trace over the path DOF and generate the states used in our study (BS stands for beam splitter). Quartz plates of various thickness have been used to produce $\rho^{\downarrow}(q)_{AB}$ and $\rho^{W}(\epsilon)_{AB}$. We also show the analyzers $D_j(j = A,B)$ needed for QST. Each D_j is made of the cascade of a QWP, an HWP, and a polarizing beam splitter (PBS). The signal then enters a photodetector.

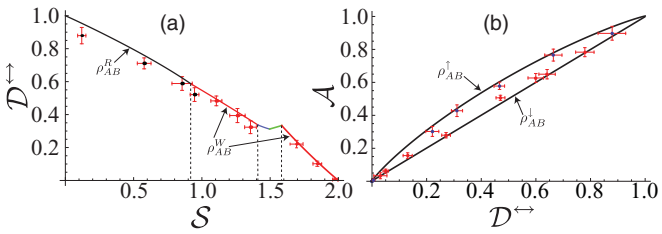

FIG. 2. (Color online) (a) Exploration of the $\mathcal{D}^{\leftrightarrow}$-vs-$\mathcal{S}$ plane. The solid line shows the MNCMS boundary (b) Experimental comparison between AMID and $\mathcal{D}^{\leftrightarrow}$. The solid lines embody the bounds to $\mathcal{A}$ at set values of $\mathcal{D}^{\leftrightarrow}$. Both panels show experimental states and associated uncertainties.

the difference between total and classical mutual information and has the prerequisites to be a *bona fide* measure of QCs [18].

We are in a position to discuss the results of our experiment by first addressing the $(\mathcal{D}^{\leftrightarrow},\mathcal{S})$ plane. As shown in Refs. [10,13], when $\mathcal{D}^{\leftrightarrow}$ and $\mathcal{S}$ are taken as quantitative figures of merit for QCs and global mixedness, the class of MNCMS consists of four families of states, all of the form

$$\rho^{X}_{AB} = \begin{bmatrix} \rho_{11} & 0 & 0 & \rho_{14} \\ 0 & \rho_{22} & \rho_{23} & 0 \\ 0 & \rho^{*}_{23} & \rho_{33} & 0 \\ \rho^{*}_{14} & 0 & 0 & \rho_{44} \end{bmatrix}, \text{ with } \sum_{j} \rho_{jj} = 1. \quad (2)$$

The low-entropy region $\mathcal{S} \in [0,0.9231)$ pertains to the rank-3 states ρ^{R}_{AB} embodying MEMS for the relative entropy of entanglement [11]:

$$\rho^{R}_{AB} = \frac{1-a+r}{2}|\Phi^{+}\rangle\langle\Phi^{+}| + \frac{1-a-r}{2}|\Phi^{-}\rangle\langle\Phi^{-}| + a|01\rangle\langle 01|, \quad (3)$$

with $0 \leqslant a \leqslant 1/3$ and r a proper function of a [10]. In Eq. (3) we have used the Bell state $|\Phi^{\pm}\rangle \equiv |\phi^{\pm}(1/2)\rangle_{AB}$. States ρ^{R}_{AB} span the leftmost trait in Fig. 2(a). Next comes the family of Werner states

$$\rho^{W}_{AB}(\epsilon) = (1-\epsilon)|\Phi^{+}\rangle_{AB}\langle\Phi^{+}| + \epsilon\mathbb{1}_4/4, \quad (4)$$

which occupy the entropic sector $\mathcal{S} \in [0.9231,1.410)$ for $\epsilon \in [0.225,0.426)$ and the high-entropy region of $\mathcal{S} \in [1.585,2]$ for $\epsilon \in [0.519,1]$. Such boundaries are clearly shown in Fig. 2(a). Evidently, two more families belong to the MNCMS boundary [cf. the two traits corresponding to $\mathcal{S} \in [1.410,1.585)$]. Such states are currently out of our grasp due to the small entropy window they belong to, which challenges the tunability of the VNE achievable by our method.

It is worth noticing that quantum discord and AMID share the very same structure of MNCMS, which can thus be rightfully regarded as the two-qubit states whose QCs are maximally robust against state mixedness. This class of states are thus set to play a key role in realistic implementations of quantum information schemes based on nonclassicality of correlations as a resource [4,5]. Currently, the interest in designing practical schemes for the exploitation of such features is enormous. The sharing of such a class of states by the two measures addressed here pushes to set a hierarchy between $\mathcal{A}$ and $\mathcal{D}^{\leftrightarrow}$; a point along the lines of the quantitative comparisons between different measures of entanglement applied to mixed two-qubit states [20].

Such a relationship is given in Fig. 2(b), where the solid lines show that AMID embodies an upper bound to $\mathcal{D}^{\leftrightarrow}$ and is in agreement with the latter in identifying classical-classical states with no QCs. Any physical two-qubit state lives between the lower bound with $\mathcal{A} = \mathcal{D}^{\leftrightarrow}$ and the upper bound. A full characterization of such boundaries is possible and can be thoroughly checked by means of a numerical exploration of the $\mathcal{A}$-vs-$\mathcal{D}^{\leftrightarrow}$ plane [10]. Clearly, the lower bound in the AMID-discord plane is spanned by pure states of variable entanglement (for pure states $\mathcal{A} = \mathcal{D}^{\leftrightarrow}$). However, it also accommodates both the Werner states and the family

$$\rho^{\downarrow}_{AB}(q) = (1-q)|\Phi^{+}\rangle_{AB}\langle\Phi^{+}| + q|\Phi^{-}\rangle_{AB}\langle\Phi^{-}|, \quad (5)$$

where $q \in [0,0.5]$, while the upper bound is spanned by

$$\rho^{\uparrow}(\epsilon,p)_{AB} = (1-\epsilon)|\phi^{+}(p)\rangle_{AB}\langle\phi^{+}(p)| + \epsilon|01\rangle_{AB}\langle 01| \quad (6)$$

for values of (ϵ,p) satisfying a transcendental equation [10]. Starting from the state $|\xi\rangle_{AB}$, we have spanned the MNCMS boundary in Fig. 2(a) and the frontiers in the $(\mathcal{A},\mathcal{D}^{\leftrightarrow})$ plane.

Generation of $\rho^{\uparrow}_{AB}$. This class serves as an ideal platform for the description of the experimental method pursued to achieve the remaining states addressed in our study. By tracing out the path DOF in $|\xi\rangle_{AB}$ and using the correspondence between physical states and logical qubits $|H\rangle \to |0\rangle$, $|V\rangle \to |1\rangle$, the density matrix for state $\rho^{\uparrow}(\epsilon,p)$ is achieved. The trace over the path DOF is performed by matching the left and right side of the modes coming from the four-hole mask in Fig. 1(a) on a beam splitter [indicated as BS in panel (b) of the same figure]. When the difference between left and right paths is larger than the photon coherence time, an incoherent superposition of $|\phi^{+}(p)\rangle_{AB}$ and $|HV\rangle_{AB}$ is achieved. The values of the pairs (ϵ,p) determining the experimental states [shown as blue dots in Fig. 2(b)] are given in Table I, together with their uncertainties. The values $(\epsilon,p) = (0,0.5)$ and $(\epsilon,p) = (0.2,1)$ correspond to the case of a pure state (having $\mathcal{A} = \mathcal{D}^{\leftrightarrow} = 1$) and a completely mixed state (with $\mathcal{A} = \mathcal{D}^{\leftrightarrow} = 0$), respectively.

Generation of $\rho^{\downarrow}_{AB}$. The family embodied by $\rho^{\downarrow}_{AB}(q)$ can also be generated starting from the resource state $|\xi\rangle_{AB}$. By selecting only the correlated modes $|r\ell\rangle_{AB}$ from the four-hole

TABLE I. Experimental values of the parameters entering $\rho^{\uparrow}(\epsilon,p)$ and their uncertainties.

	Value and Uncertainty					
ϵ	0.00 ± 0.01	0.05 ± 0.01	0.10 ± 0.01	0.15 ± 0.01	0.18 ± 0.01	0.20 ± 0.01
p	0.50 ± 0.02	0.70 ± 0.01	0.80 ± 0.01	0.90 ± 0.01	0.95 ± 0.02	0.99 ± 0.02

mask and setting QWP_2 at 0° (so that $p = 1/2$ is fixed), we generate the Bell state $|\Phi^+\rangle_{AB}\langle\Phi^+| \equiv \rho^{\downarrow}(q = 0)$. By inserting a birefringent quartz plate of proper thickness on the path of one of the two correlated modes, we controllably affect the coherence between the $|HH\rangle$ and $|VV\rangle$ states of polarization. Several quartz plates of different thickness ℓ_q have been used to transform $|\Phi^+\rangle$ into $\rho^{\downarrow}(q)$. The value of q is related to the parameter $C = (\Delta n)\ell_q/(c\tau_{\rm coh})$, where $\tau_{\rm coh}$ is the coherence time of the emitted photons and Δn is the difference between ordinary and extraordinary refraction indices in the quartz. We skip inessential details and simply state that $q = 1/2$ ($q \to 0$) for $C \gg 1$ ($C \to 0$).

Generation of $\rho^{R,W}$. Our source of ρ^R and the Werner state uses the setup previously described for the states $\rho^{\uparrow}_{AB}(\epsilon, p)$. By setting $p = 1/2$ and by adding a decoherence between $|HH\rangle$ and $|VV\rangle$ (related to the parameter r) as previously explained, we can obtain ρ^R_{AB} from $\rho^{\uparrow}_{AB}$. As for ρ^W_{AB}, while we have already addressed the method used to generate the $|\Phi^+\rangle_{AB}\langle\Phi^+|$ component of the state, it is worth mentioning how to get the $\mathbb{1}_4$ contribution. This has been obtained by inserting a further HWP [HWP_2 in Fig. 1(a)] on the $|\ell\rangle_A$ mode and rotating both HWP_1 and HWP_2 at 22.5° so as to generate $|\ell r\rangle_{AB}|++\rangle_{AB}$. By using two quartz plates longer than $\tau_{\rm coh}$ and of different thickness, we obtained a fully mixed state of modes $|\ell r\rangle_{AB}$. The quartz plates introduce decoherence on each photon state. By matching the two correlated-mode pairs on a BS, ρ^W_{AB} is achieved.

To ascertain the properties of the states discussed above, we have used QST [14] so as to obtain the physical density matrices and quantify $\mathcal{D}^{\leftrightarrow}$, $\mathcal{S}$, and $\mathcal{A}$. The Pauli operators needed to implement the QST have been measured by using standard polarization analyzers and two detectors [cf. the inset in Fig. 1(b)]. Integrated systems given by gradient-index (GRIN) lenses and single-mode fibers [21] have been used to collect the radiation after the QST setup and send it to the detectors $D_{A,B}$.

Discussion and conclusions. Excellent agreement between the theoretical expectations and experimental results has been found for both the navigation in the space of MNCMS and the quantitative confirmation of the relation between $\mathcal{A}$ and $\mathcal{D}^{\leftrightarrow}$. As seen in Fig. 2, almost the whole class of maximally nonclassical states has been explored, with the exception of a technically demanding (yet interesting) region. Remarkably, the whole upper bound in the $(\mathcal{A}, \mathcal{D}^{\leftrightarrow})$ plane has been scanned by an experiment that has produced an ample wealth of interesting states. Technically, this has been achieved by engineering a 4-qubit hyperentangled state. In particular, we exploit the path as an ancillary resource to obtain the desired states encoded in polarization. Our analysis reports a full navigation in the space of general QCs at set values of global entropy, thus going beyond analogous investigations performed on entanglement [12]. We hope that our efforts will spur further interest in the study of the interplay between mixedness and nonclassicality.

We thank V. Rosati for the contributions given in realizing the experiment. MP thanks G. Adesso and D. Girolami for fruitful discussions. This work was supported by the FARI project 2010 of Sapienza Università di Roma, and the UK EPSRC (EP/G004579/1).

[1] E. Schrödinger, Proc. Cambridge Philos. Soc. **31**, 555 (1935).
[2] R. Horodecki *et al*., Rev. Mod. Phys. **81**, 865 (2009).
[3] H. Ollivier and W. H. Zurek, Phys. Rev. Lett. **88**, 017901 (2001); L. Henderson and V. Vedral, J. Phys. A **34**, 6899 (2001).
[4] A. Datta, A. Shaji, and C. M. Caves, Phys. Rev. Lett. **100**, 050502 (2008).
[5] B. P. Lanyon, M. Barbieri, M. P. Almeida, and A. G. White, Phys. Rev. Lett. **101**, 200501 (2008).
[6] P. Giorda and M. G. A. Paris, Phys. Rev. Lett. **105**, 020503 (2010); G. Adesso and A. Datta, *ibid*. **105**, 030501 (2010).
[7] L. Mazzola, J. Piilo, and S. Maniscalco, Phys. Rev. Lett. **104**, 200401 (2010).
[8] D. Cavalcanti *et al*., Phys. Rev. A **83**, 032324 (2011); V. Madhok and A. Datta, *ibid*. **83**, 032323 (2011).
[9] S. Luo, Phys. Rev. A **77**, 042303 (2008).
[10] D. Girolami, M. Paternostro, and G. Adesso, J. Phys. A **44**, 352002 (2011).
[11] W. J. Munro, D. F. V. James, A. G. White, and P. G. Kwiat, Phys. Rev. A **64**, 030302 (2001); T. Wei *et al*., *ibid*. **67**, 022110 (2003).
[12] N. A. Peters *et al*., Phys. Rev. Lett. **92**, 133601 (2004); M. Barbieri, F. DeMartini, G. DiNepi, and P. Mataloni, *ibid*. **92**, 177901 (2004); G. Puentes, A. Aiello, D. Voigt, and J. P. Woerdman, Phys. Rev. A **75**, 032319 (2007).
[13] A. Al Qasimi and D. F. V. James, Phys. Rev. A **83**, 032101 (2011); F. Galve, G. L. Giorgi, and R. Zambrini, *ibid*. **83**, 012102 (2011).
[14] D. F. V. James, P. G. Kwiat, W. J. Munro, and A. G. White, Phys. Rev. A **64**, 052312 (2001).
[15] M. Barbieri, C. Cinelli, P. Mataloni, and F. DeMartini, Phys. Rev. A **72**, 052110 (2005).
[16] A. Chiuri *et al*., Phys. Rev. Lett. **105**, 250501 (2010).
[17] G. Vallone, E. Pomarico, F. DeMartini, P. Mataloni, and M. Barbieri, Phys. Rev. A **76**, 012319 (2007).
[18] M. Piani, P. Horodecki, and R. Horodecki, Phys. Rev. Lett. **100**, 090502 (2008).
[19] B. M. Terhal *et al*., J. Math. Phys. **43**, 4286 (2002); D. P. DiVincenzo, M. Horodecki, D. W. Leung, J. A. Smolin, and B. M. Terhal, Phys. Rev. Lett. **92**, 067902 (2004).
[20] S. Virmani and M. B. Plenio, Phys. Lett. A **268**, 31 (2000).
[21] A. Rossi, G. Vallone, A. Chiuri, F. DeMartini, and P. Mataloni, Phys. Rev. Lett. **102**, 153902 (2009).